Pergamon

SCIENCE DIRECT®

Tetrahedron 59 (2003) 10567–10574

TETRAHEDRON

Methyl methacrylate polymerization at samarium(II)-grafted MCM-41

Reiner Anwander,* Iris Nagl, Clemens Zapilko and Markus Widenmeyer

Anorganisch-chemisches Institut, Technische Universität München, D-85747 Garching, Lichtenbergstrasse 4, München, Germany

Received 11 June 2003; accepted 16 July 2003

Abstract—Sm(II)-modified periodic mesoporous silica (PMS), $Sm[N(SiHMe_2)_2]_2(THF)_x$@MCM-41, was used for the synthesis of Sm(II) alkyl, alkoxide, and indenyl surface species via secondary ligand exchange. The performance of the novel Sm(II)-based organometallic–inorganic hybrid materials as initiators for the graft polymerization of methyl methacrylate (MMA) is reported. All of the Sm(II) hybrid materials including the new PMMA–PMS composites were characterized via N_2 physisorption, elemental analysis, FTIR spectroscopy, and scanning electron microscopy (SEM). The organic–inorganic composites revealed complete pore blockage as well as enrichment and strong adhesion of the polymer at the exterior of the porous silica material.

1. Introduction

Divalent samarium compounds, particularly $SmI_2(THF)_2$ [Kagan's reagent], display unique one-electron-reductants in organic synthesis.[1] Moreover, $SmI_2(THF)_2$ as well as Sm(II) organometallics are excellent initiators for α-olefin and ring-opening polymerization.[2,3] For example, Cp^*_2-$Sm(THF)_2$ initiates the living polymerization of MMA according to a unprecedented bisinitiator anionic coordination mechanism via a methyl methacrylate radical intermediate.[4] Also, non-metallocene derivatives of Sm(II) such as oxygen-only-ligated $Sm(OC_6H_2tBu_2\text{-}2,6\text{-}Me\text{-}4)_2(THF)_3$[5] and *N*/*O*-coordinated $((2\text{-}PyridylCH(Ph))_2\text{-}SiMe_2)Sm(THF)_2$[6] were recently shown to produce polymethyl methacrylate (PMMA) in an efficient manner. On the other hand, organic–inorganic composites such as PMMA-functionalized silica are discussed as advanced materials for, e.g. controlled adhesion, lubricity, and biocompatibility.[7] We thought that Sm(II) modified periodic mesoporous silicas such as $Sm[N(SiHMe_2)_2]_2(THF)_x$@ PMS are interesting candidates for studying an intrapore-initiated graft polymerization of MMA.[8] Note that surface confinement seems to be a viable route to affect the product selectivity of Sm(II)-mediated transformations. Inclusion and extrusion polymerization reactions are known polymerization techniques to control the stereochemistry and morphology of polymers.[9] Meanwhile, there have been several reports on the controlled polymerization within mesoporous silica of MCM-41 and MCM-48 topology.[10,11] These studies include the free radical polymerization of MMA within MCM-41[12] as well as the ring-opening polymerization of lactones and L,L-lactide by Al-MCM-41[13] and Sn-HMS.[14] Furthermore, MCM-41-supported zirconocene,[15–20] titanocene,[21] and chromium acetyl acetonate[22] were shown to polymerize ethylene or propylene in the presence of MAO as a cocatalyst and when activated thermally, respectively.

2. Results and discussion

2.1. Synthesis and characterization of differently ligated Sm(II) surface species

$Sm[N(SiHMe_2)_2]_2(THF)_x$@MCM-41 (**2a** and **2b**) were synthesized according to a previously reported procedure from $Sm[N(SiHMe_2)_2]_2(THF)_x$ and dehydrated pore-enlarged MCM-41 materials **1a** and **1b** (Scheme 1).[8] According to this procedure, approximately 2.4 mmol of samarium(II) species per 1 g of **1** immobilized which corresponds to a relatively high surface coverage of ca. 1.34 and 1.24 Sm(II)/nm^2, respectively. For comparison, the maximum silanol surface sites available for these materials were determined as 1.69 (**1a**) and 1.73 SiOH/nm^2 (**1b**) via tetramethyldisilazane silylation.[23] Characterization of the Sm(II) hybrid materials **2** through FTIR spectroscopy not only revealed complete consumption of all of the surface silanol groups but also the importance of the 'SiH' moiety as a spectroscopic probe (Fig. 1). The presence of metal-bonded silylamide ligands is clearly indicated in the IR spectrum, the SiH vibration area being dominated by a

Keywords: samarium(II); mesoporous silica MCM-41; surface organometallic chemistry (SOMC); alkyl ligand; alkoxide ligand; indenyl ligand; methyl methacrylate (MMA); polymerization; organoaluminum reagents.

* Corresponding author. Tel.: +49-89-289-13096; fax: +49-89-289-13473; e-mail: reiner.anwander@ch.tum.de

0040–4020/$ - see front matter © 2003 Elsevier Ltd. All rights reserved.
doi:10.1016/j.tet.2003.07.018

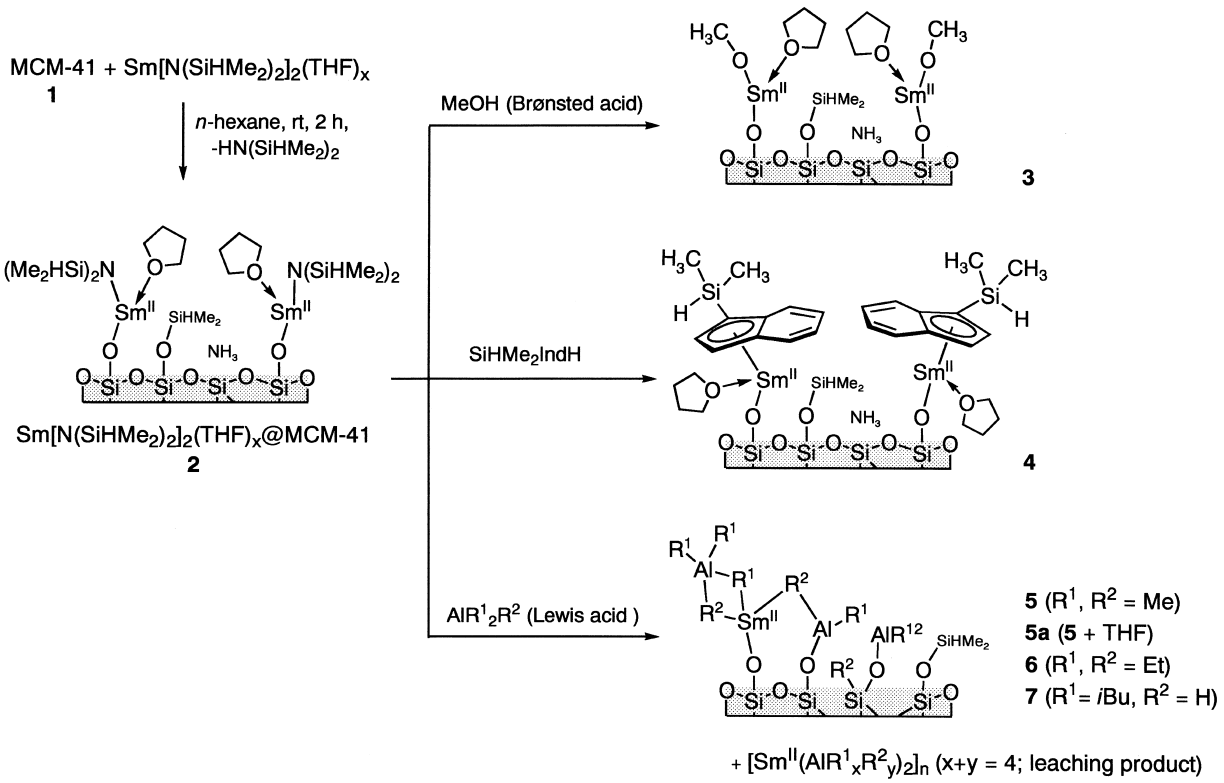

Scheme 1. Proposed surface species of surface-mediated ligand exchange reactions: *n*-hexane, rt, 18 h.

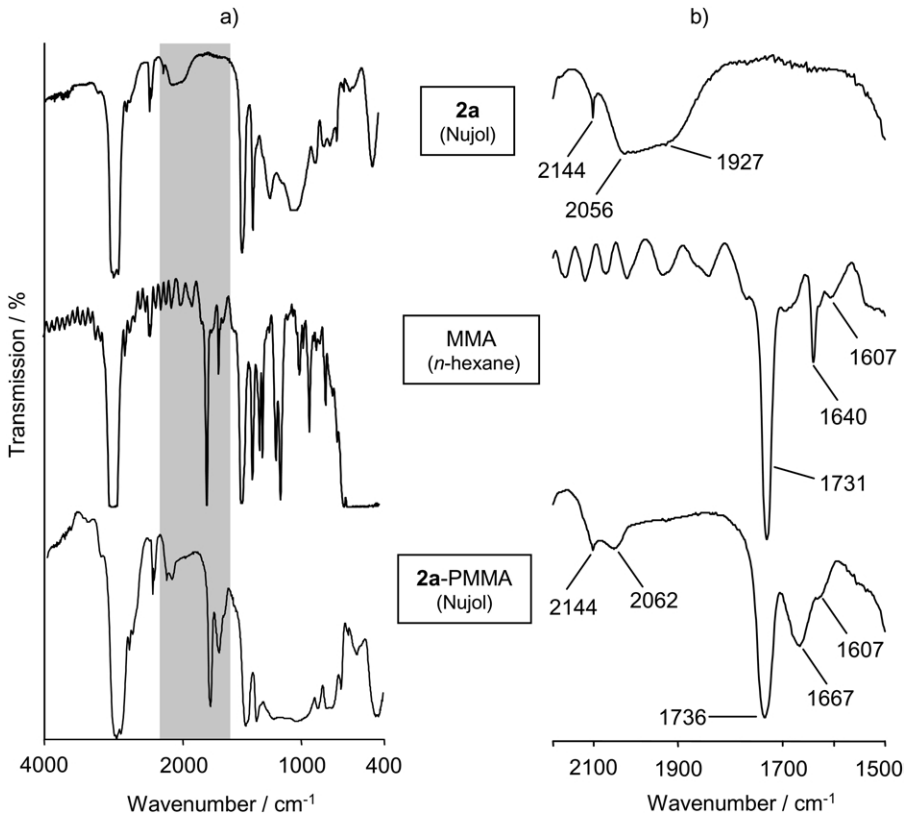

Figure 1. IR spectra of materials $Sm[N(SiHMe_2)_2]_2(THF)_x$@MCM-41 (**2a**), MMA, and **2a**-PMMA: (a) full spectra; (b) areas of Si-H and C═O/C═C stretching vibrations.

broad band at 2030 cm^{-1} and a pronounced shoulder at 1920 cm^{-1} assignable to Sm···SiH β-agostic interactions.

Surface organometallic chemistry (SOMC) involving silylamide ligand exchange at the Sm(II) centers was carried out by procedures well-known in solution organometallic chemistry.[24] Silylamide/methanol exchange yielding material **3** was accomplished according to Scheme 1 using a slight excess of alcohol regarding the Sm(II) surface centers. Such SOLnC (surface organolanthanide chemistry) gives access to a 'small ligand chemistry' of oxophilic and electrophilic metal centers, unknown in solution chemistry due to agglomeration phenomena.[11,25] Material **4** featuring a bulky dimethylsilyl-substituted indenyl ligand was obtained via silylamide/indene exchange.[26] The course of these surface-mediated ligand exchange reactions could be easily monitored by using FTIR spectroscopy and by exploiting the distinct ν(Si–H) vibration. Quantitative ligand exchange and release of silylamine is indicated by a complete disappearance of the strong and broad band at 2030 cm^{-1}, with the weaker band at 2144 cm^{-1} ($\equiv$SiOSiHMe$_2$ species originating from in situ surface silylation) still being present (Fig. 1). The characteristic Si–H stretching vibration of the newly introduced indenyl ligand in material **4** could be identified at 2122 cm^{-1}. The carbon contents of samples **3** and **4** also clearly indicate ligand exchange as envisioned (Table 1), while the molar amount of immobilized metal did not change (approximately 20 wt% corresponding to 1.3 mmol of Sm(II) per 1 g of support).

The alkylation reactions shown in Scheme 1 using excess of organoaluminum reagents were multifunctional in nature. Addition of $AlMe_3$ to a black suspension of Sm[N(SiHMe$_2$)$_2$]$_2$(THF)$_x$@MCM-41 (**2b**) in *n*-hexane generated a pink material **5**, which could be separated from a colorless *n*-hexane solution containing $AlMe_3$(THF) and {Me$_2$Al[μ-N(SiHMe$_2$)$_2$]$_2$}$_2$ as soluble co-products. Although isolation of the latter aluminum amide unequivocally proved the silylamide/alkyl exchange at the Sm(II) center, the formation of insoluble [Sm(AlMe$_4$)$_2$]$_x$ as a possible leaching product could not be excluded. Therefore, we conducted a separate experiment by reacting Sm[N(SiHMe$_2$)$_2$]$_2$(THF)$_x$ with $AlMe_3$ in *n*-hexane solution. This reaction produced, in analogy with ytterbium(II) chemistry,[27] [Sm(AlMe$_4$)$_2$]$_x$ as a pink *n*-hexane-insoluble powder which formed a purple THF solution. When hybrid material **5** was suspended in THF, leaching of a considerable amount of Sm(II) was indicated by a dark purple solution. Material **5** was treated several times with THF until the washings were colorless. Hybrid material **5a** obtained from these washings was still pink. Accordingly, the $AlEt_3$- and HAl*i*Bu$_2$-reactions produced in addition to dark-brown hybrid materials **6** and **7** *n*-hexane-soluble black leaching products [Sm(AlR$_4$)$_2$]$_x$ (R=Et, *i*Bu), the tetraethylaluminate derivatives of which (**6b**) could be identified by NMR spectroscopy. In order to afford complete removal of the leaching products from samples **6** and **7**, the organoaluminum treatment was conducted twice. We propose that the organoaluminum reagent surface-disrupt most of the monopodally anchored Sm(II) centers, $\equiv$SiOSm[N(SiHMe$_2$)$_2$](THF)$_x$, while the stronger surface-bonded bipodally anchored Sm(II) centers, ($\equiv$SiO)$_2$Sm (not shown in Scheme 1), withstand the alkylation procedure. This is in sharp contrast to Ln(III)-silylamide-grafted PMS materials (Ln=Sc, Y, La) which did not reveal any significant leaching upon treatment with $AlMe_3$.[28] Destabilization of the Sm(II) surface species could also result from the reaction of excess organoaluminum reagent with strained siloxane bridges as indicated in the cartoon of Scheme 1. It also can be assumed that in analogy with the alkylated Ln(III) materials, the Sm(II)-containing samples **5a**, **6**, and **7** feature a high aluminum content. Complete silylamide/alkyl ligand exchange in materials **5a**, **6**, and **7** was indicated by the disappearance of the Si-H stretching vibration at 2030 cm^{-1} due to metal-bonded silylamide ligands. The band at 2144 cm^{-1} was still present although organoaluminum compounds are capable of disrupting this type of siloxane bridges.[29]

The nitrogen adsorption/desorption isotherms shown in Figure 2 are also consistent with the surface reactions

Table 1. Analytical data, surface area, pore volume, and effective mean pore diameter

Material[a]	Wt% C	wt% Sm	a_s[b] ($m^2\ g^{-1}$)	V_p[c] ($cm^3\ g^{-1}$)	d_p[d] (nm)
MCM-41 (**1a**)	–	–	1080	1.25	3.7
MCM-41 (**1b**)	–	–	1165	1.20	3.9
[MCM-41]Sm[N(SiHMe$_2$)$_2$]$_x$(THF)$_y$ (**2a**)	10.80	–[e]	420	0.34	2.75
2a-PMMA	37.19	–[e]	~30	–	–
2a-PMMA-THF	33.97	–[e]	–	–	–
[MCM-41]Sm[N(SiHMe$_2$)$_2$]$_x$(THF)$_y$ (**2b**)	10.75	19.6	410	0.34	2.8
[MCM-41]Sm(OMe)$_x$(THF)$_y$ (**3**)[f]	8.02	22.1	510	0.46	2.95
[MCM-41]Sm(C$_9$H$_6$SiHMe$_2$)$_x$(THF)$_y$ (**4**)[g]	18.68	20.0	190	0.16	2.4–3.0[h]
2b+$AlMe_3$+THF (**5a**)	12.50	–[e]	530	0.49	3.0
2b+$AlEt_3$ (**6**)	14.73	–[e]	430	0.39	2.9
6+$AlEt_3$ (**6a**)	14.72	–[e]	450	0.40	2.8
2b+HAl*i*Bu$_3$ (**7**)	12.90	–[e]	410	0.34	2.7

[a] Pretreatment temperature: 250°C, 3 h, 10^{-3} Torr for **1a** and **1b**; 25°C, 5 h, 10^{-3} Torr for **2**–**6**.
[b] Specific BET surface area.
[c] BJH desorption cumulative pore volume of pores between 1.5 and 6.5 nm diameter.
[d] Pore diameter according to the maximum of the BJH pore size distribution.
[e] Samarium content not determined.
[f] Obtained from **2b**.
[g] Obtained from **2a**.
[h] Extremely broad pore size distribution featuring several maxima.

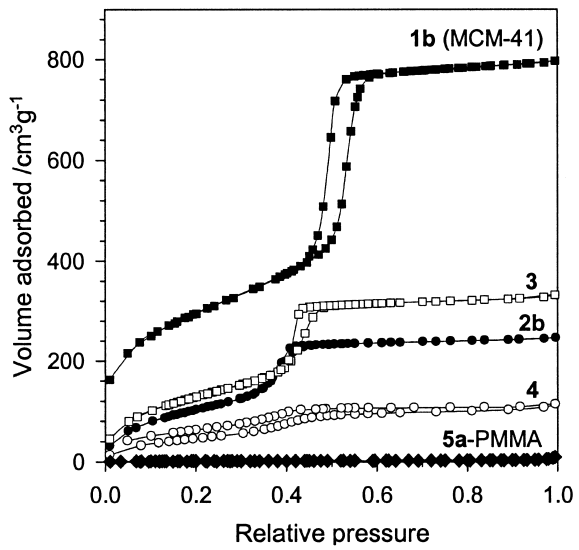

Figure 2. Nitrogen adsorption/desorption isotherms at 77.4 K of the parent MCM-41 material **1b** (–■–; 10^{-3} Torr, >3 h, 250°C) and modified organic–inorganic hybrids **2b** (–●–; **1b**+{Sm[N(SiHMe$_2$)$_2$]$_2$(THF)$_x$}; 10^{-3} Torr, >5 h, rt), **3** (–□–; **2b**+HOMe; 10^{-3} Torr, >5 h, rt), **4** (–○–; **2b**+$C_9H_7SiHMe_2$; 10^{-3} Torr, >5 h, rt), and **5a**-PMMA (–◆–; **2b**+$AlMe_3$+THF+methyl methacrylate (MMA); 10^{-3} Torr, >5 h, rt); cf. Table 1.

proposed in Scheme 1, clearly indicating the filling of the mesopores. All of the organometallic/inorganic hybrid materials under study display mesoporosity (Table 1) and type-IV isotherms.[30] The silylamide-grafted samples **2** exhibited a drastically reduced pore volume (ΔV_p=ca. 0.88 cm^3 g^{-1}) and pore diameter (Δd_p=ca. 1.0 nm) in comparison with the parent MCM-41 materials **1**. In material **3**, these pore parameters increased by 0.12 cm^3 g^{-1} and 0.2 nm, respectively, which is in accordance with the displacement of the N(SiHMe$_2$)$_2$ ligand by the sterically less demanding methoxide group. Exchange of the silylamide ligand by the more bulky indenyl ligand $C_9H_6SiHMe_2$ afforded material **4** featuring dramatically decreased surface area and pore volume (ca. 50%). Interestingly, the isotherm of material **4** seems to be not reversible at relative pressures below 0.2. The appearance of such a low-pressure hysteresis has been reported recently by us[23] and Jaroniec et al.[31] Material **5a**, which was obtained by consecutive treatment of material **2b** with $AlMe_3$ and THF, features pore characteristics similar to those of material **3**. The isotherms of $AlEt_3$– and HAl*i*Bu$_2$-treated materials **6** and **7**, respectively, showed only slight changes relative to those of their synthetic precursor **2b** exhibiting pore diameters of d_p=2.7–2.8 nm and pore volumes of V_p=0.34–0.40 cm^3 g^{-1} depending on the steric peculiarities of the individual alkyl ligands (Table 1). Repeated treatment of $AlEt_3$-alkylated material **6** with $AlEt_3$ to yield **6a** did not further change the pore parameters.

2.2. Graft polymerization of MMA

Sm(II)-initiated olefin polymerizations in homogeneous solution are well-documented.[3] It was also shown that Sm(II) organometallics with ancillary ligands such as Cp* or aryloxides effectively initiate the living polymerization of methyl methacrylate (MMA).[4–6] Correspondingly, materials **2**–**7** featuring Sm(II) surface centers with either (≡Si–O–), silylamide, methoxide, indenyl, and alkyl ligands were studied as initiators for the polymerization of MMA. First of all, we examined the reactivity of the Sm(II) silylamide-grafted material **2b** toward MMA (50 equiv. of MMA, regarding the metal content, *n*-hexane, rt, 18 h). Upon addition of MMA, the color of dark brown **2b** changed to light brown. The composite material **2b**-PMMA which was obtained after several washings and drying under vacuum, exhibited a high carbon content (+ca. 300%, Tables 1 and 2). The IR spectrum of **2b**-PMMA showed typical bands attributable to the carbonyl moieties of PMMA (ν(CO)=1731 cm^{-1}, Fig. 1). Additionally, the displacement of surface-confined Sm(II)···SiH β-agostic interactions by Sm-MMA/enolate coordination was revealed by the disappearance of the agostic shoulder at 1927 cm^{-1} and formation of a new band centered at 1667 cm^{-1}. Only a small amount of PMMA (ca. 3%, M_n=9800, M_n/M_w=1.6) could be separated by prolonged treatment of material **2b**-PMMA with THF (18 h, 50°C). This is in accordance with enolate linkages between the Sm(II) centers and the polymer which cannot be disrupted by THF and/or a strong adhesion of the polar polymer onto the polar surface. The use of 500 equiv. MMA and toluene as a solvent did not increase the polymer yield.

In order to investigate the implications of the local ligand environment of the Sm(II) initiation sites for the polymerization, hybrid materials **3**–**7** were examined under identical conditions. The compositions of the resulting PMMA-PMS materials are listed in Table 2. It is clear that material **3** with the small methoxide ligands at the Sm(II) centers gave a higher amount of polymer than its synthetic silylamide-ligated precursor **2b**. From calculations of the maximum amount of PMMA which can be placed in the pores of each material it is also clear that at least 75% of the polymer has to be outside the pores. Also, the alkylated materials **5a**, **6**, and **7** showed an enhanced reactivity with the $AlMe_3$-treated sample being the most efficient. In contrast, the Sm(II) centers in material **4** seem to be less accessible due to the presence of sterically bulky indenyl ligands. Noteworthy, also the parent unmodified material **1b** produced a significant amount of PMMA (0.432 g per 1 g of MCM-41).[32] Nitrogen physisorption isotherms representatively shown for material **5a**-PMMA revealed a low surface area (~30 m^2 g^{-1}) and the apparent total loss of pore

Table 2. Composition of PMMA-PMS materials[a]

Material	wt% C	PMMA[b] (g)	Max. amount of PMMA inside the pore system[c] (g)
1b-PMMA	18.11	0.432	1.416
2b-PMMA	34.55	1.246	0.401
3-PMMA	40.82	1.914	0.543
4-PMMA	22.85	0.263	0.189
5a-PMMA	41.12	2.429	0.578
6-PMMA	37.21	1.350	0.460
7-PMMA	37.55	1.857	0. 401

[a] Conditions: in toluene, precat/MMA (mol/mol)=1:500, MMA/solvent (v/v)=1/10; polymerization time=18 h; polymerization temperature=30°C.
[b] MMA content in g of the composite material referred to 1 g of MCM-41 material, after drying (25°C, 10^{-3} Torr, 3 h).
[c] Maximum amount of intrapore PMMA, calculated from V_p and d_{PMMA}=1.18 g cm^{-3}.

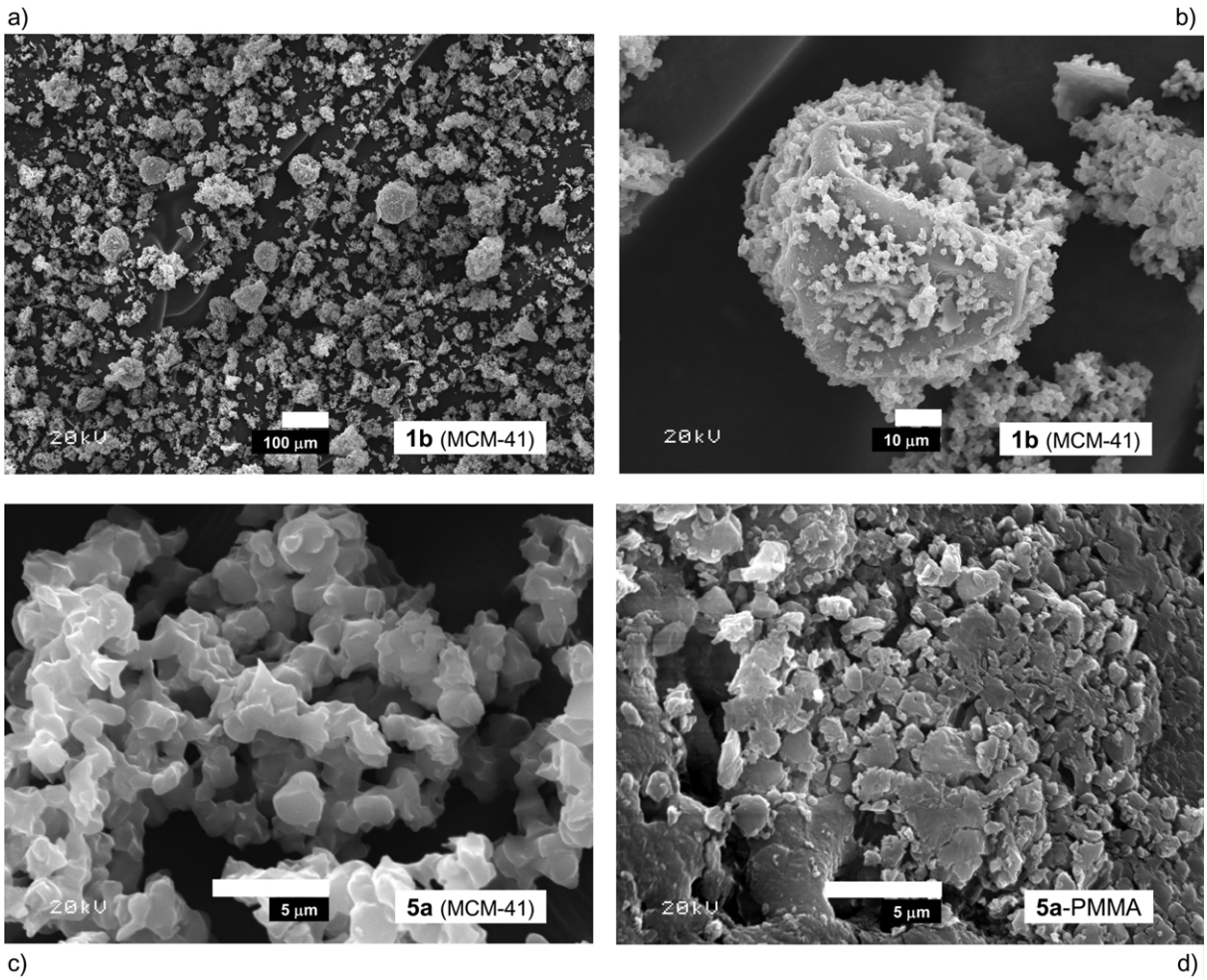

Figure 3. Scanning electron micrographs of MCM-41 **1b** (a, b; after template removal), $AlMe_3$-alkylated material **5a** (c), and composite material **5a**-PMMA (d, after methyl methacrylate polymerization).

volume (Table 1, Fig. 2). This indicates either complete pore filling or blockage of the PMMA–PMS composites.

Representative scanning electron micrographs (SEMs) of the parent MCM-41 material **1b** show an irregular size (0.5–100 μm) and various shapes (hexagons, spheres) of the primary particles (Fig. 3(a) and (b)). The SEM images of material **5a** proved that grafting of Sm(II) silylamide and subsequent alkylation with organoaluminum reagents did not significantly affect the morphology of the sample, that is, the interconnected network of aggregated particles stayed intact (Fig. 3(c)). Note that surface-mediated ligand exchange has a dramatic effect on the local environment of the metal center (Scheme 1). The SEM photographs of composite material **5a**-PMMA show that the PMS primary particles are covered and stuck together with PMMA (Fig. 3(d)). Although quenching with methanol should have disrupted the Sm(III) enolate(polymer) bonds as indicated by the disapperance of the IR band at 1667 cm^{-1} and appearance of broad OH bands at 3621 and 3440 cm^{-1} (not shown), we have not been able to efficiently separate the polymer from the porous silica material by treatment with either THF/50°C or $CHCl_3$/70°C. In the case of material **6**-PMMA the chloroform treatment gave a sufficient amount of polymer for characterization (M_n=50500, M_n/M_w=6.7).

There is certainly some room for speculations about the polymerization mechanism, however, if the Sm(II) surface centers display the preferred initiation sites, surface species as shown in Figure 4 could be proposed.

Oxidation of the Sm(II) centers by MMA is clearly indicated by the color change of the hybrid materials and has to involve the initial formation of Sm(III)-bonded MMA radicals. The generation of surface-confined ketyl radicals has been unequivocally proven for the transformation of fluorenone to fluorenol.[8] Additionally, the reversible formation of surface bonded ketyl radicals has been also

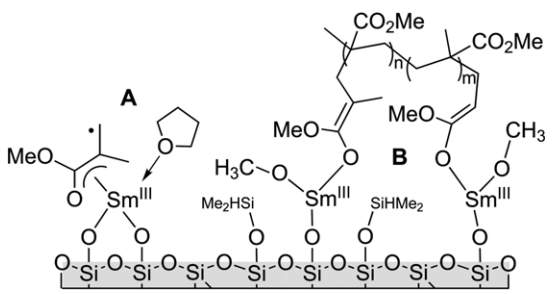

Figure 4. Proposed surface species **A** (bipodal Sm(III)) and **B** (monopodal Sm(III)), obtained by addition of excess of MMA to methoxide-exchanged material **3**.

shown for δ,ε-unsaturated ketones.[33] Unlike soluble molecular Sm(III)-MMA˙ radical species which are supposed to couple after the addition of one MMA monomer, producing a dinuclear bis(enolate) bisinitiator system,[4] the surface confined radical anions **A**, Sm(III)-MMA˙, are proposed to add the next few MMA monomers in a radical manner. Coupling of the MMA radical anions to afford species **B** cannot occur after addition of the first MMA monomer due to the steric separation of the surface-bonded Sm centers. Anionic coordination polymerization can proceed after radical dimerization through the double bond termini of the Sm(III) enolates. The PMMA produced inside the pores is most likely oligomeric in nature due to the high population of Sm(II) surface sites on the inner surface and due to space confinement. Longer polymer chains are most likely formed at Sm centers located on the outer surface and at the pore entrances. The overall low yield of PMMA can be interpreted by MMA polymerization preferentially starting at the outer surface and at the pore entrances. Strong adhesion of the polymer to the outer surface will prevent new monomers from approaching the enolate initiation sites, particularly those located on the inner surface.

3. Conclusions

Surface organometallic chemistry was applied to generate the first Sm(II) alkoxide, indenyl, and alkyl surface species via ligand exchange at mesoporous $Sm[N(SiHMe_2)_2]_2(THF)_x$@MCM-41. Interestingly, Sm(II) grafting and subsequent ligand exchange did not markedly change the morphology and the microstructure of the samples. Such Sm(II)-modified organometallic–inorganic hybrid materials initiate the graft polymerization of methyl methacrylate, possibly via a radical-initiated anionic coordination polymerization mechanism involving sterically unsaturated surface-confined samarium enolate moieties. The local environment of the Sm(II) surface centers (coordination sphere) decisively affects their reactivity and, hence, the efficiency of MMA polymerization. Hybrid materials featuring the 'smallest' ligands (methyl, methoxy) acted as the best initiators for graft polymerization. The PMMA-PMS composites revealed complete pore filling or blockage of the pore entrances as indicated by N_2 physisorption and scanning electron microscopy. The polymer enriched and strongly binds at the exterior of the porous silica, that is, prolonged solvent extraction was unsuccessful for the separation of polymer from the host material. We are currently examining several routes in order better to control the inclusion/extrusion polymerization of rare-earth metal-grafted mesoporous silicas comprising (i) utilization of partially presilylated PMS host materials implicating a lower Ln surface population, (ii) use of unfunctionalized α-olefins and lactones as monomers, and (iii) gas phase polymerization.

4. Experimental

4.1. General

The Sm(II) hybrid materials were synthesized with rigorous exclusion of air and moisture, using glovebox techniques (MB Braun MB150B-G-II; <1 ppm O_2, <1 ppm H_2O, argon atmosphere). *n*-Hexane was purified by using Grubbs columns.[34] Toluene and THF were predried and distilled from Na/K alloy (benzophenone ketyl) under argon. C_6D_6 was obtained from Deutero GmbH, degassed, dried over Na/K alloy for 24 h, and filtered. MCM-41 samples **1a** and **1b** were synthesized according to the literature.[35] After calcination (N_2: 540°C, 5 h, heating rate 1.5°C min^{-1}; air: 540°C, 5 h) and dehydration (280°C, 10^{-5} Torr, 4 h, heating rate 1°C min^{-1}) the parent materials **1a** and **1b** were characterized by FTIR spectroscopy, powder X-ray diffraction and nitrogen physisorption at 77.4 K (Table 1, Fig. 1), and stored in a glovebox. $Sm[N(SiHMe_2)_2]_2(THF)_n$ was prepared according to the literature.[36] For the preparation of $Sm[N(SiHMe_2)_2]_2(THF)_x$@MCM-41 (**2**), $Sm[N(SiHMe_2)_2]_2(THF)_n$ (ca. 2.5 mmol per 1 g of dehydrated MCM-41) was added as a *n*-hexane solution to a suspension of **1** in *n*-hexane at ambient temperature.[8] After 1 h the hybrid material was separated and dried in vacuum (10^{-3} Torr, 5 h). Trimethylaluminum, triethylaluminum, diisobutylaluminumhydride (1 M solution in *n*-hexane), and methanol (99.8%, anhydrous) were purchased from Aldrich and used as received. $SiHMe_2C_9H_7$ was synthesized according to the literature.[37] Methyl methacrylate was dried using a method described previously.[38] IR spectra were recorded on a Perkin–Elmer 1650-FTIR spectrometer as Nujol mulls sandwiched between CsI plates. NMR spectra were performed on a JEOL-JMN-GX 400 instrument (400 MHz, ^1H; 100.54 MHz, ^{13}C). All spectra were recorded in C_6D_6 at ambient temperature unless otherwise noted. Elemental analyses were performed in the microanalytical laboratory of the institute. Nitrogen physisorption measurements were performed on an ASAP 2010 volumetric adsorption apparatus (Micromeritics) at 77 K [$a_m(N_2, 77\ K) = 0.162\ nm^2$]. Prior to analysis the samples were outgassed at ambient temperature for 5 h under vacuum (about 10^{-3} Torr) unless otherwise noted in Table 1. The specific surface area was determined by means of the BET method. The pore size distribution was obtained on the basis of the BJH method using the Kelvin equation to calculate the mean pore diameter d_p.[30] The SEM images were recorded on a JEOL-JSM-5900 LV instrument (20 kV) after coating with a gold film.

4.2. General prodedure for SOMC/ligand exchange at $Sm[N(SiHMe_2)_2]_2(THF)_x$@MCM-41 (2)

In a glovebox, *n*-hexane solutions of $AlMe_3$, $AlEt_3$, DIBAH, MeOH, and $C_9H_7SiHMe_2$ were added to materials $Sm[N(SiHMe_2)_2]_2(THF)_x$ at MCM-41 (**2**) suspended in 10 mL of *n*-hexane. After stirring for 18 h, the reaction mixtures were centrifuged. The resulting powders were washed several times with *n*-hexane until the *n*-hexane fractions became colorless (3–4×10 mL) and the materials were dried in vacuo for at least 5 h. The *n*-hexane fractions were also collected to examine any leaching products.

4.2.1. Materials 2a and 2b. Compound **2a** was synthesized from **1a**. Anal. found: C, 10.80; H, 2.70; N, 2.13. Compound **2b** was synthesized from **1b**. Anal. found: C, 10.75; H, 2.49; N, 1.94; Sm, 19.6. IR: $\tilde{\nu}$=2144w, 2034m, 1920m (sh) (ν(Si–H)), 1301w, 1223m, 1155m, 1076vs, 896m, 834w, 766w, 722m, 560w, 460s cm^{-1}.

4.2.2. Material 3. 0.156 g dark-brown powder, from 0.200 g **1b** and 0.020 mL (0.48 mmol) methanol; no metal-containing *n*-hexane-soluble leaching product. Anal. found: C, 8.02; H, 2.03; N, 0.26; Sm, 22.1. IR: $\tilde{\nu}$=2144vw, 1600w, 1238s, 1074s, 803s, 722m, 454s cm^{-1}.

4.2.3. Material 4. 0.210 g dark-brown powder, from 0.200 g **1a** and 0.085 g (0.49 mmol) dimethylindenylsilane; no metal-containing *n*-hexane-soluble leaching product. Anal. found: C, 18.68; H, 3.30; N, 1.23; Sm, 20.0. IR: $\tilde{\nu}$=2144vw, 2122m, 1340w, 1328w, 1245s, 1070vs, 899m, 831m, 765m, 697m, 626w, 439vs cm^{-1}.

4.2.4. Material 5a. 0.157 g pink powder, from 0.200 g **1b** and 0.208 g (2.88 mmol) $AlMe_3$ and after washing with THF; 0.125 g THF-soluble samarium-containing purple oily residue. Anal. found: C, 12.50; H, 2.55; N, 0.53. IR: $\tilde{\nu}$=2144vw, 1240s, 1065s, 915m, 807m, 721m, 686m, 446s cm^{-1}.

4.2.5. Material 6. 0.173 g dark-brown powder, from 0.200 g **1b** and 2.88 mL (2.88 mmol, 1 M in *n*-hexane) $AlEt_3$; 0.160 g *n*-hexane-soluble samarium-containing black crystalline residue. Anal. found: C, 14.73; H, 3.13; N, 0.65. IR: $\tilde{\nu}$=2144vw, 1243s, 1066s, 900w, 808w, 722m, 444s cm^{-1}. Leaching product: $[Sm(AlEt_4)_2]_x$ (**6a**): ^1H NMR (400 MHz, C_6D_6, 25°C): δ −1.39 (s, CH_3), −38.9 (s, CH_2). ^{13}C NMR (68 MHz, C_6D_6, 25°C): δ 30.1 (s, CH_3), −14.9 (m, CH_2). IR: $\tilde{\nu}$=1409w, 1301w, 1188w, 1168w, 1107m, 982s, 945s, 846w, 648s, 585s, 534m, 497m, 463m cm^{-1}. Anal. calcd for $C_{16}H_{40}Al_2Sm$: C, 44.0; H, 9.23. Found: C, 44.5; H, 9.50.

4.2.6. Material 7. 0.196 g dark-brown powder, from 0.200 g **1b** and 2.88 mL (2.88 mmol, 1 M in *n*-hexane) DIBAH; 0.196 g *n*-hexane-soluble samarium-containing purple oily residue. Anal. found: C, 12.90; H, 2.77; N, 1.33. IR: $\tilde{\nu}$=2144vw, 2030vw, 1243s, 1066s, 900w, 808w, 444s cm^{-1}.

4.3. Polymerization of methyl methacrylate (MMA)

For the synthesis of the organic–inorganic composites, ca. 500 equiv. of MMA (0.130 mol, regarding the Sm(II) content, corresponding to ca. 0.2 mol% catalyst; the Sm(II) content of the alkylated samples **5**–**7** was estimated as 12%) were added to a suspension of 0.200 g of hybrid material in 5 mL of toluene at ambient temperature. After the solution was stirred for 18 h at ambient temperature, the polymerization was terminated by the addition of 100 mL methanol and stirred for 1 h (outside the glovebox). The resulting white composites were collected by filtration and dried under reduced pressure (Table 2). Few samples of the polymethyl methacrylate were analyzed by means of gel permeation chromatography (calibrated with standard polystyrene samples) and differential scanning calorimetry.

Acknowledgements

Financial support from the Deutsche Forschungsgemeinschaft and the Fonds der Chemischen Industrie is gratefully acknowledged. M.W. thanks the Fonds der Chemischen Industrie for a fellowship (with participation of the Bundesministerium für Bildung, Wissenschaft, Forschung und Technologie). The authors thank Professor Wolfgang A. Herrmann for his continued support and Dr J. Froh for obtaining the SEM images.

References

1. (a) Molander, G. A.; Harris, C. R. *Chem. Rev.* **1996**, *96*, 307–338. (b) Kagan, H. B.; Namy, J.-L. *Top. Organomet. Chem.* **1999**, *2*, 155–198.
2. (a) Narita, M.; Nomura, R.; Tomita, I.; Endo, T. *Macromolecules* **1998**, *31*, 2774–2778. (b) Gosho, A.; Nomura, R.; Tomita, I.; Endo, T. *Macromolecules* **1998**, *31*, 3388–3390. (c) Tanaka, M.; Sudo, A.; Sanda, F.; Endo, F. *Chem. Commun.* **2000**, 2503–2504.
3. For reviews, see: (a) Yasuda, H. *Top. Organomet. Chem.* **1999**, *2*, 255–283. (b) Anwander, R. *Applied Homogeneous Catalysis with Organometallic Compounds*; Cornils, B., Herrmann, W. A., Eds.; VCH: Weinheim, 2002; Vol. 2, pp 974–1014. (c) Hou, Z.; Wakatsuki, Y. *Coord. Chem. Rev.* **2002**, *231*, 1–22.
4. (a) Boffa, L. S.; Novak, B. M. *Macromolecules* **1994**, *27*, 6993–6995. (b) Boffa, L. S.; Novak, B. M. *Tetrahedron* **1997**, *53*, 15367–15396.
5. Nodono, M.; Tokimitsu, T.; Makino, T. *Macromol. Chem. Phys.* **2003**, *204*, 877–884.
6. Ihara, E.; Koyama, K.; Yasuda, H.; Kanehisa, N.; Kai, Y. *J. Organomet. Chem.* **1999**, *574*, 40–49.
7. (a) Boven, G.; Oosterling, M. L. C. M.; Challa, G.; Schouten, A. J. *Polymer* **1990**, *31*, 2377–2383. (b) Matsuda, T.; Saito, N.; Sugawara, T. *Macromolecules* **1996**, *29*, 7446–7451. (c) Ejaz, M.; Yamamoto, S.; Ohno, K.; Tsujii, Y.; Fukuda, T. *Macromolecules* **1998**, *31*, 5934–5936. (d) Zhao, B.; Brittain, W. J. *J. Am. Chem. Soc.* **1999**, *121*, 3557–3558. (e) Ingall, M. D. K.; Joray, S. J.; Duffy, D. J.; Long, D. P.; Bianconi, P. A. *J. Am. Chem. Soc.* **2000**, *122*, 7845–7846.
8. Nagl, I.; Widenmeyer, M.; Grasser, S.; Köhler, K.; Anwander, R. *J. Am. Chem. Soc.* **2000**, *122*, 1544–1545.
9. Miyata, M. *Comprehensive Supramolecular Chemistry*; Reinhoudt, D. N., Ed.; Pergamon: Oxford, 1996; Vol. 10, pp 557–582.
10. Tajima, K.; Aida, T. *Chem. Commun.* **2000**, 2399–2412.
11. Anwander, R. *Chem. Mater.* **2001**, *13*, 4419–4438.
12. For, PMMA–PMS composite materials obtained via free radical polymerization (T>70°C), see: (a) Llewellyn, P. L.; Ciesla, U.; Becher, H.; Stadler, R.; Schüth, F.; Unger, K. K. *Stud. Surf. Sci. Catal.* **1994**, *84*, 2013–2020. (b) Ng, S. M.; Ogino, S.; Aida, T. *Macromol. Rapid Commun.* **1997**, *18*, 991–996. (c) Möller, K.; Bein, T.; Fischer, R. X. *Chem. Mater.* **1998**, *10*, 1841–1852. (d) Möller, K.; Bein, T.; Fischer, R. X. *Chem. Mater.* **1999**, *11*, 665–673.
13. Kageyama, K.; Ogino, S.; Aida, T.; Tatsumi, T. *Macromolecules* **1998**, *31*, 4069–4073.
14. Abdel-Fattah, T. M.; Pinnavaia, T. J. *Chem. Commun.* **1996**, 665–666.
15. Ko, Y. S.; Han, T. K.; Park, J. W.; Woo, S. I. *Macromol. Rapid Commun.* **1996**, *17*, 749–758.
16. (a) Tudor, J.; O'Hare, D. *Chem. Commun.* **1997**, 603–604. (b) O'Brien, S.; Tudor, J.; Maschmeyer, T.; O'Hare, D. *Chem. Commun.* **1997**, 1905–1906.

17. (a) Van Looveren, L. K.; Geysen, D. F. M. C.; Vercruysse, K. A. L.; Wouters, B. H. J.; Grobet, P. J.; Jacobs, P. A. *Angew. Chem.* **1998**, *110*, 540–543, *Angew. Chem., Int. Ed.* **1998**, *37*, 517–520. (b) Van Looveren, L. K.; Geysen, D. F. M. C.; Vercruysse, K. A. L.; Wouters, B. H. J.; Grobet, P. J.; Jacobs, P. A. *Stud. Surf. Sci. Catal.* **1998**, *117*, 477–484.
18. Sano, T.; Doi, K.; Hagimoto, H.; Wang, Z.; Uozumi, T.; Soga, K. *Chem. Commun.* **1999**, 733–734.
19. Rahiala, H.; Beurroies, I.; Eklund, T.; Hakala, K.; Gougeon, R.; Trens, P.; Rosenholm, J. B. *J. Catal.* **1999**, *188*, 14–23.
20. Lee, K.-S.; Oh, C.-G.; Yim, J.-H.; Ihm, S.-K. *J. Mol. Catal.* **2000**, *159*, 301–308.
21. (a) Kageyama, K.; Tamazawa, J.; Aida, T. *Science* **1999**, *285*, 2113–2115. (b) Tajima, K.; Ogawa, G.; Aida, T. *J. Polym. Sci. A: Polym. Chem.* **2000**, *38*, 4821–4825.
22. (a) Rao, R. R.; Weckhuysen, B. M.; Schoonheydt, R. A. *Chem. Commun.* **1999**, 445–446. (b) Weckhuysen, B. M.; Rao, R. R.; Pelgrims, J.; Schoonheydt, R. A.; Bodart, P.; Debras, G.; Collart, O.; Van Der Voort, P.; Vansant, E. F. *Chem. Eur. J.* **2000**, *6*, 2960–2970.
23. Anwander, R.; Nagl, I.; Widenmeyer, M.; Engelhardt, G.; Groeger, O.; Palm, C.; Röser, T. *J. Phys. Chem. B* **2000**, *104*, 3532–3544.
24. Anwander, R. *Top. Organomet. Chem.* **1999**, *2*, 1–61.
25. Anwander, R.; Palm, C. *Stud. Surf. Sci. Catal.* **1998**, *117*, 413–420.
26. For use of this indenyl ligand in homogeneously performed silylamine elimination reactions, see: Klimpel, M. G.; Herrmann, W. A.; Anwander, R. *Organometallics* **2000**, *19*, 4666–4668.
27. Klimpel, M. G.; Anwander, R.; Tafipolsky, M.; Scherer, W. *Organometallics* **2001**, *20*, 3983–3992.
28. Nagl, I.; Widenmeyer, M.; Herdtweck, E.; Raudaschl-Sieber, G.; Anwander, R. *Microporous Mesoporous Mater.* **2001**, *44–45*, 311–319.
29. (a) Jenkner, H. *Z. Naturforsch.* **1959**, *14B*, 133. (b) Mehrotra, R. C.; Rai, A. K. *Polyhedron* **1991**, *10*, 1967. (c) Feher, F. J.; Budzichowski, T. A.; Weller, K. J. *Polyhedron.* **1993**, *12*, 591.
30. Sing, K. S. W.; Everett, D. H.; Haul, R. A. W.; Moscou, L.; Pierotti, R. A.; Rouquérol, J.; Siemieniewska, T. *Pure Appl. Chem.* **1985**, *57*, 603–619.
31. Jaroniec, C. P.; Kruk, M.; Jaroniec, M.; Sayari, A. *J. Phys. Chem. B* **1998**, *102*, 5503.
32. For comparison, the $AlMe_3$-alkylated Sc(III)-grafted MCM-41 reported in Ref. 28 produced 1.693 g PMMA per 1 g of MCM-41.
33. (a) Anwander, R.; Nagl, I.; Hölemann, A.; Reißig, H.-U. Unpublished results. (b) Nagl, I. Ph.D. Thesis, Technische Universität München, 2002.
34. Grubbs, R. H.; Pangborn, A. B.; Giardello, M. A.; Rosen, R. K.; Timmers, F. J. *Organometallics* **1996**, *15*, 1518–1520.
35. The mesoporous silicas were synthesized according to slightly modified literature procedures, pore-expanded materials were employed better to apply the BJH pore size analysis to the Sm(II) hybrid materials. Mesitylene was used as a swelling reagent for the preparation of pore-expanded MCM-41 (**1**): (a) Beck, J. S.; Vartuli, J. C.; Roth, W. J.; Leonowicz, M. E.; Kresge, C. T.; Schmitt, K. D.; Chu, C. T.-W.; Olson, D. H.; Sheppard, E. W.; McCullen, S. B.; Higgins, J. B.; Schlenker, J. L. *J. Am. Chem. Soc.* **1992**, *114*, 10834–10843. (b) Widenmeyer, M. Ph.D. Thesis, Technische Universität München, 2001.
36. Nagl, I.; Scherer, W.; Tafipolsky, M.; Anwander, R. *Eur. J. Inorg. Chem.* **1999**, 1405–1407.
37. Eppinger, J.; Spiegler, M.; Hieringer, W.; Herrmann, W. A.; Anwander, R. *J. Am. Chem. Soc.* **2000**, *122*, 3080–3096.
38. Allen, R. D.; Long, T. E.; McGrath, J. E. *Polym. Bull.* **1986**, *15*, 127.